Spin-symmetry conversion in methyl rotors induced by tunnel resonance at low temperature

B. Zhang, C. Sun, A. M. Alsanoosi, A. Aibout, and A. J. Horsewill

Citation: The Journal of Chemical Physics **140**, 084302 (2014); doi: 10.1063/1.4865835
View online: http://dx.doi.org/10.1063/1.4865835
View Table of Contents: http://scitation.aip.org/content/aip/journal/jcp/140/8?ver=pdfcov
Published by the AIP Publishing

Spin-symmetry conversion in methyl rotors induced by tunnel resonance at low temperature

B. Zhang,[1] C. Sun,[1,a)] A. M. Alsanoosi,[2] A. Aibout,[3] and A. J. Horsewill[1,b)]
[1]*School of Physics and Astronomy, University of Nottingham, Nottingham NG7 2RD, United Kingdom*
[2]*Physics Department, King Abdulaziz University, P.O. Box 80203, Jeddah 21589, Saudi Arabia*
[3]*Laboratoire de Spectroscopie des Materiaux, Université de Mostaganem, B.P. 227, Mostaganem 2700, Algeria*

(Received 19 December 2013; accepted 3 February 2014; published online 24 February 2014)

Field-cycling NMR in the solid state at low temperature (4.2 K) has been employed to measure the tunneling spectra of methyl (CH_3) rotors in phenylacetone and toluene. The phenomenon of tunnel resonance reveals anomalies in ^{1}H magnetization from which the following tunnel frequencies have been determined: phenylacetone, $\nu_t = 6.58 \pm 0.08$ MHz; toluene, $\nu_{t(1)} = 6.45 \pm 0.06$ GHz and $\nu_{t(2)} = 7.07 \pm 0.06$ GHz. The tunnel frequencies in the two samples differ by three orders of magnitude, meaning different experimental approaches are required. In phenylacetone the magnetization anomalies are observed when the tunnel frequency matches one or two times the ^{1}H Larmor frequency. In toluene, doping with free radicals enables magnetization anomalies to be observed when the tunnel frequency is equal to the electron spin Larmor frequency. Cross-polarization processes between the tunneling and Zeeman systems are proposed and form the basis of a thermodynamic model to simulate the tunnel resonance spectra. These invoke space-spin interactions to drive the changes in nuclear spin-symmetry. The tunnel resonance lineshapes are explained, showing good quantitative agreement between experiment and simulations. © *2014 AIP Publishing LLC*. [http://dx.doi.org/10.1063/1.4865835]

I. INTRODUCTION

Analogous to *ortho*- and *para*-hydrogen, methyl groups, CH_3, exhibit nuclear spin isomerism. Classified as "quantum rotors," these symmetrical systems exhibit their quantum mechanical properties in a number of ways. For example, the wave-like characteristics of the CH_3 rotor give rise to quantum tunneling through a potential barrier that hinders rotation.[1–3] Additionally, the anti-symmetry principle that underpins the Pauli Exclusion Principle (PEP) leads to an entanglement of space and nuclear spin variables.[1] This partitions the states into classes with different spin-symmetry that can have a profound influence on the behavior of the quantum rotor. This includes the thermodynamics of the system which is particularly relevant to this investigation. To induce a change in CH_3 nuclear spin-symmetry involves simultaneous changes in spatial and spin state, requiring a magnetic interaction coupling space and spin. Such interactions may not be abundant, particularly at low temperature, and quantum rotor systems are often characterized by thermal reservoirs that are only very weakly coupled to their environment.

The issue of spin-symmetry and nuclear spin isomerism is one that has been of recent interest in a number of contexts. For example, experiments on methyl systems that exhibit phenomena related to the Haupt-effect[4] have been reported by a number of groups. Upon dissolution and a rise in sample temperature, Ludwig *et al.*[5] observe hyperpolarization effects that compete with dynamic nuclear polarization. Similarly inducing a sudden rise in temperature in CH_3 containing samples, Icker *et al.*[6,7] have reported anti-phase multiplet components in the high-resolution NMR spectrum of ^{13}C-γ-picoline. A theoretical framework successfully describing such quantum rotor-induced polarization has recently been presented by the group of Levitt in Southampton.[8] The H_2O molecule also exhibits nuclear spin-isomerism and recent advances in "molecular surgery" techniques in synthetic organic chemistry have enabled isolated H_2O molecules to be studied, entrapped inside a C_{60} cage. Here the conversion between *ortho*-H_2O and *para*-H_2O has been followed in real time.[9] Additionally, it is noted that related principles apply in the physics and chemistry of long-lived nuclear singlet states.[10,11] Common to all these systems is the requirement for space-spin interactions to induce transitions between states with different spin-symmetry.

For CH_3 the tunneling and spin-symmetry principles are intimately linked and magnetic resonance is well placed to investigate such systems since the technique is rich in interactions that connect space and spin. In this investigation on CH_3 rotors the emphasis has been to use electron spin and nuclear spin interactions to drive changes in nuclear spin-symmetry. This gives rise to resonant features in nuclear magnetization that occur at particular magnetic fields where there is a cross-polarization between tunneling and Zeeman spin states. Energy flows between various weakly coupled thermal reservoirs and the phenomenon is described as "tunnel resonance."[3,12–20] The experiments are conducted at low temperature and the tunneling spectra are recorded using solid state NMR.

a)Present address: Department of Physical Science, Dalian University, No. 10, Xuefu Avenue, Economic Technological Development Zone, 116622 Dalian, Liaoning Province, China.
b)Author to whom correspondence should be addressed. Electronic mail: a.horsewill@nottingham.ac.uk

In this investigation we have explored the dynamical and thermodynamical properties of methyl groups in toluene (methylbenzene: $C_6H_5CH_3$) and phenylacetone (1-phenylpropan-2-one: $C_6H_5CH_2(CO)CH_3$). These two materials possess methyl tunneling frequencies that differ by three orders of magnitude but we investigate the extent to which their thermodynamic properties are similar.

The rotation of a methyl group is hindered by a potential barrier determined by the electrostatic interactions of the hydrogen atoms with the crystalline molecular environment. The barrier shares the three-fold symmetry of the CH_3 rotor, although in general it can also possess six-fold and higher harmonic components. At low temperature the methyl group undergoes coherent quantum tunneling through the barrier, characterized by the ground state tunneling frequency ν_t. The latter is exponentially dependent on the barrier height V_3. There is a hierarchy of tunneling states, comprising pairs with A and E spin-symmetry reflecting the irreducible representations of the symmetry group C_3. In the ground tunneling state, the lowest lying level has A-symmetry and is a nuclear spin quartet with total spin 3/2. This is paired with two degenerate states with E_a and E_b symmetry which are each nuclear spin doublets with spin 1/2. In the ground tunnelling state the A-E splitting is equal to $h\nu_t$, Fig. 1.

Experimentally the phenomenon of tunnel resonance can be brought about by tuning the magnetic field so that the Larmor frequency of either a nuclear or an electron spin is equal to ν_t. When the tunneling and Zeeman systems are brought into resonance in this way then A-E conversion pathways become available, releasing energy and allowing the A and E spin-symmetry species to equilibrate. These transitions involve changes in spin state so the tunnel resonance reveals itself in the form of field-dependent anomalies in nuclear magnetization. In previous electron spin tunnel resonance work on CH_3 systems, unpaired electrons have been incorporated in two principle ways, (a) by doping with paramagnetic metal ions, as in Cu^{2+} doped zinc acetate[21] and (b) by using γ-irradiation to produce free-radicals as in ammonium acetate[20] and 4-methyl-2,6-ditertiarybutylphenol.[18] In these experiments the tunnel resonance lineshapes often reveal dynamic nuclear polarization (DNP) of the ^{1}H spins. Previous work on nuclear spin tunnel resonance has revealed the level-crossings that occur within the manifold of tunneling-Zeeman states, as in acetone.[16]

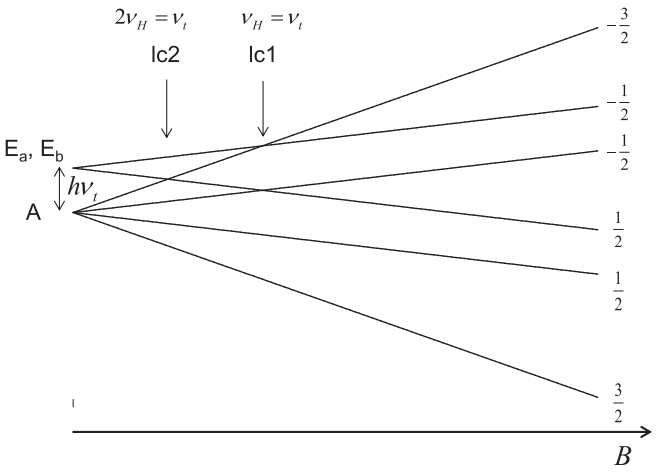

FIG. 1. The B-field dependence of the manifold of CH_3 tunneling-Zeeman levels showing the tunneling splitting, $h\nu_t$ and the level crossings lc1 and lc2. The spin-symmetry species A and E are a nuclear spin quartet of total spin 3/2 and a nuclear spin doublet of total spin 1/2, respectively. The E species comprises degenerate E_a and E_b species.

In this paper we shall describe two types of tunnel resonance experiment. In one, toluene has been doped with small concentrations of the free radical DPPH (2,2-di-phenyl-1-picrylhydrazyl) and electron spin resonance (ESR) transitions mediate the coupling between A and E spin-symmetry species. In the second, nuclear spin transitions in pure phenylacetone mediate the spin-symmetry conversion.

II. EXPERIMENTAL

Experiments were conducted in the solid state at low temperature using a TecMag Apollo pulsed NMR spectrometer and home-built cryogenic probe operating at 36.7 MHz. At this frequency, the ^{1}H spins are resonant at the field $B_{nmr} = 0.862$ T.

In these experiments we shall variously refer to the ^{1}H magnetization, M_z, the ^{1}H spin polarization, P_Z, and the inverse Zeeman temperature, β_Z. The Curie Law applies and the three quantities are proportional to each other. A measurement of the equilibrium ^{1}H magnetisation M_0 at a given field and temperature provides the means to calibrate the NMR signal and as appropriate, experimental values are reported in terms of $P_Z = (n_+ - n_-)/(n_+ + n_-)$ or M_z ($n_\pm$ designates the population of the state $m_I = \pm\frac{1}{2}$).

The tunnel resonance experiments were conducted with variable recovery field B_r using the Nottingham field-cycling NMR magnet system.[22] The latter comprises a low inductance superconducting solenoid that is permanently connected using low loss leads to its power supply rated at 160 A, ±15 V. In these experiments, the field switching rate was typically 3 T s^{-1}. The tunnel resonance experiment is based on a saturation-recovery pulse sequence incorporating rapid field-cycling, Fig. 2. At the beginning of the sequence the field is raised from zero to the ^{1}H resonance field where any residual magnetization is reduced to zero using a saturation comb. The field is then switched to the recovery field B_r where the polarization is evolved for the period τ_r. Finally the field is switched back to the ^{1}H resonance field where M_z is measured with a single pulse of duration 2 μs before the field is reset to zero at the end of the sequence. The tunnel resonance spectrum is recorded by repeating the sequence with sequential increments (or decrements) in B_r and plotting M_z.

The field-cycling magnet system incorporates a variable temperature He cryostat that provides sample temperatures in the range $4.2 \le T \le 300$ K with stability $\Delta T < 0.05$ K. The samples of phenylacetone (98%) and toluene (99.99%) were obtained commercially and used as supplied. Toluene has two crystalline forms and to obtain the stable α-form[23] the temperature was cycled in the following way. First the sample was quenched cooled to 77 K by plunging the NMR probe into liquid nitrogen. The cold probe assembly was then inserted into the helium cryostat and the temperature was raised

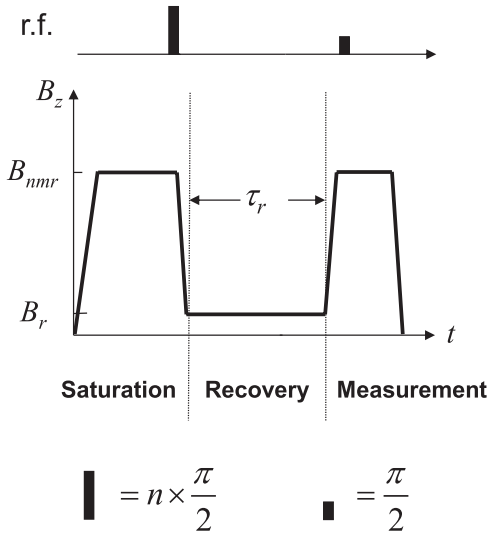

FIG. 2. The field-cycling NMR pulse sequence employed in the tunnel resonance scans.

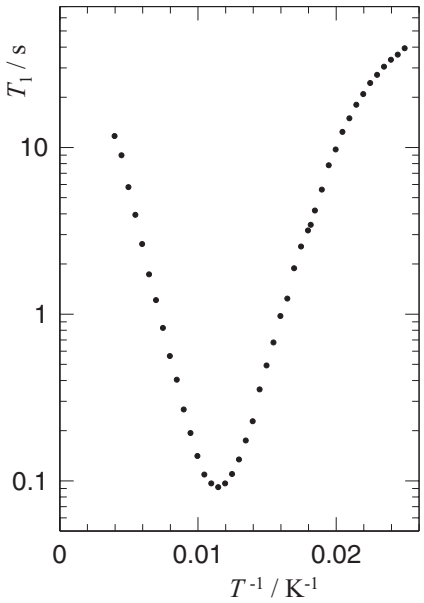

FIG. 3. The inverse temperature dependence of the ^{1}H spin-lattice relaxation time T_1 in phenylacetone measured at $\nu_H = 36.7$ MHz, $B = 0.862$ T.

to 160 K where the sample was annealed for approximately 1 h before being cooled to 4.2 K in preparation for the NMR experiments. A similar procedure was used in preparing the phenylacetone sample.

DPPH dissolves readily in toluene and the presence of the free electron spins provides an additional spin-lattice relaxation mechanism. For the tunnel resonance experiments on toluene it was undesirable for the ^{1}H T_1 to be too fast, therefore, preliminary experiments were conducted to establish the optimum concentration. For the experiments reported here, the sample of toluene was doped with approximately 4 mol.% of DPPH.

III. RESULTS

A. Phenylacetone

The inverse temperature dependence of the ^{1}H T_1 in phenylacetone recorded at fixed field, $\nu_H = 36.7$ MHz, $B = 0.862$ T, is presented in Fig. 3. A minimum is observed at 87 K. Using the correlation of Clough[24] we can estimate the ground state tunneling frequency to be of order 5 MHz which is in the range accessible to the NMR tunnel resonance technique. Phenylacetone is liquid at room temperature and when the sample was directly cooled to 4.2 K a phase with a fast spin-lattice relaxation time was typically observed. The ^{1}H T_1 could be as fast as 5 s at 4.2 K, indicating disorder in the sample. Much longer T_1 values were obtained by thermal cycling from 4.2 K to a few degrees below the melting point (258 K), then annealing for approximately 30 min and re-cooling to 4.2 K. This procedure provided a sample with ^{1}H $T_1 = 160$ s at $B = 0.178$ T. These observations suggest that thermal cycling and annealing provided a more crystalline sample.

Tunnel resonance scans of ^{1}H polarization have been made for an annealed sample in the range $B_r = 0$–0.3 T using the field-cycling NMR pulse sequence in Fig. 2. In order to pre-cool the tunnel reservoir, a tunnel resonance scan was preceded by switching the field to 1.2 T for 15 min. In Fig. 4(a), a series of ^{1}H tunnel resonance spectra are shown, recorded at 4.2 K with a variety of recovery times in the range $90 \leq \tau_r \leq 240$ s. In all spectra, the ^{1}H polarization P_Z increases systematically with increasing field in response to the Curie Law. However, all spectra exhibit two stepwise changes in P_Z that are identified with arrows. These features appear at magnetic field values that are close to the ratio 2:1 and are assigned to tunnel resonances of the CH_3 groups. They correspond to the two level (anti-) crossings at $\nu_t^{(0)} = \nu_H$ (lc1) and $\nu_t^{(0)} = 2\nu_H$ (lc2) indicated in the energy level diagram, Fig. 1. We shall return in the discussion to consider the stepwise shapes of the tunnel resonances.

To visually accentuate the influence of the level crossings on P_Z, the first derivative of the tunnel resonance spectrum is presented in Fig. 4(b). The resulting peaks more precisely identify the two level crossing fields at 0.155 ± 0.002 (lc1) and 0.077 ± 0.002 T (lc2), respectively, while also defining the range of field over which they are active. The systematic uncertainty in the B-field makes the leading contribution to the error bars. We hence determine the ground state tunneling frequency of methyl groups in phenylacetone to be $\nu_t = 6.58 \pm 0.08$ MHz.

B. Toluene doped with DPPH radicals

The methyl tunnel spectrum of toluene is known from inelastic neutron scattering (INS)[23] and comprises two tunneling splittings of 26.0 and 28.5 μeV, corresponding to physically distinguishable CH_3 groups with different barrier heights. Tunnel resonance spectra with variable relaxation time $30 \leq \tau_r \leq 70$ s are presented in Fig. 5(a). The ^{1}H magnetization data is presented as a fraction of the equilibrium magnetization at the same field, M_Z/M_0. In Fig. 5(b), a detail is shown after removal of the sloping component of the baseline, clearly showing two peak-like anomalies centered at 0.230 ± 0.002 and 0.252 ± 0.002 T,

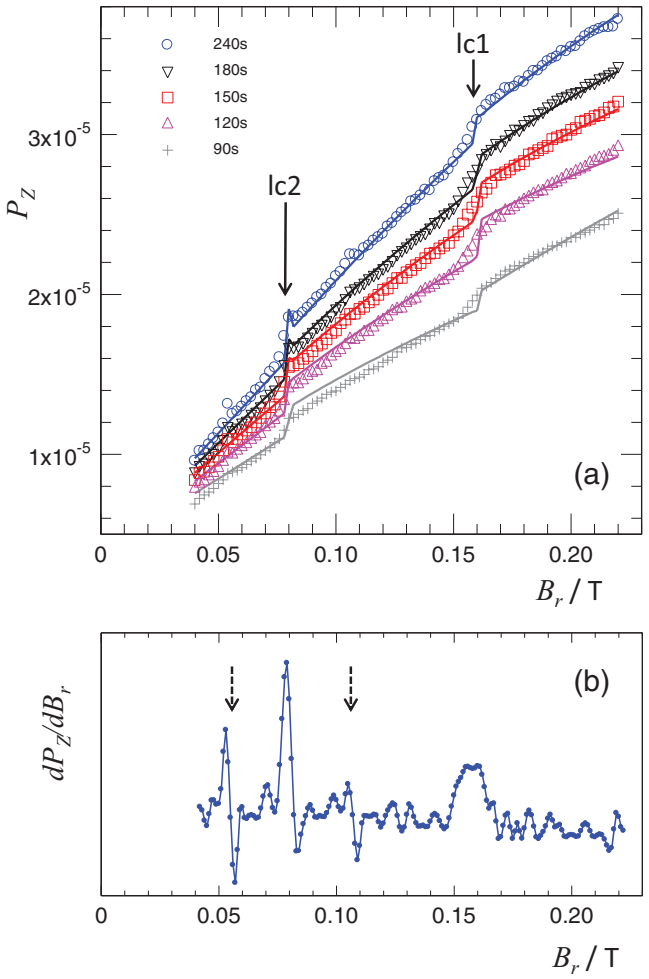

FIG. 4. The tunnel resonance spectra of phenylacetone recorded at 4.2 K with variable recovery time τ_r. (a) ^{1}H polarization P_Z and (b) the derivative dP_Z/dB_r of the spectrum. Steps in polarization are observed at the level crossings shown in Fig. 1 from which the tunnel frequency is determined, $\nu_t = 6.58 \pm 0.08$MHz. The tunnel resonance spectra are successfully reproduced using the numerical simulation described in the text (solid lines). The dashed arrows reveal additional tunnel resonance features arising from mechanical coupling between pairs of CH_3 groups.

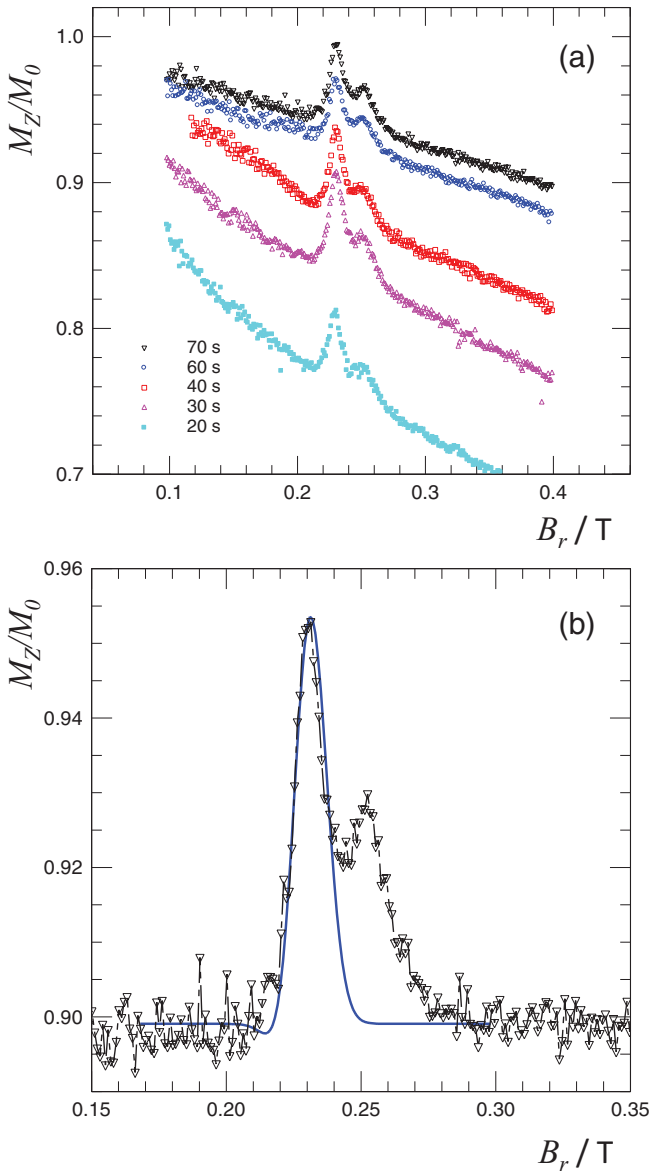

FIG. 5. The tunnel resonance spectra of DPPH-doped toluene recorded at 4.2 K with variable recovery time τ_r. (a) ^{1}H magnetization as a fraction of equilibrium magnetization at the same field, M_z/M_0, (b) highlighting the spectrum, $\tau_r = 70$ s with a sloping baseline component removed. The two peaks identify two physically distinguishable CH_3 groups with $\nu_{t(1)} = 6.45 \pm 0.06$ GHz and $\nu_{t(2)} = 7.07 \pm 0.06$ GHz. Using the numerical simulation described in the text, quantitative agreement with experiment is obtained for the tunnel resonance lineshape (solid line).

consistent with the INS spectrum. These occur when the electron Larmor frequency, $\nu_S = g\beta B/h$, matches the methyl tunnel frequency. Given $g = 2.0036$ for DPPH, the two tunneling frequencies are hence determined to be $\nu_{t(1)} = 6.45 \pm 0.06$ GHz and $\nu_{t(2)} = 7.07 \pm 0.06$ GHz. As observed in the INS spectrum, the higher frequency tunnel peak has the lower amplitude.

In this investigation, the particular interest lies in the tunnel resonance phenomenon and the lineshapes revealed in the spectrum. Electron tunnel resonance spectra reported in the literature commonly exhibit asymmetric lineshapes revealing an underlying DNP mechanism.[18–21] By contrast, in Fig. 5 the polarization effects arising from contact with the electron spin result in symmetrical peaks. The amplitude of these tunneling peaks grows with increasing τ_r as the contact time with the electron spin increases. This growth is superimposed on a background that also increases with τ_r due to spin–lattice relaxation.

In DPPH doped toluene the tunnel resonance peak amplitude is typically only 5% of the equilibrium ^{1}H magnetization, M_0. Furthermore, the magnitude of the tunnel resonance effect is unaffected by repeated scans. Both observations suggest that contact with the electron spin only marginally cools the tunneling reservoir. By contrast, in Cu^{2+} doped zinc acetate the tunnel resonance amplitudes were factors of two to four times larger than M_0.[21] However, a comparison of the tunnel resonance linewidths shows they are approximately the same in the two samples as a proportion of the tunneling frequency (approximately 7% in toluene and 10% in zinc acetate). These factors will be considered in Sec. IV in discussing the observed lineshapes.

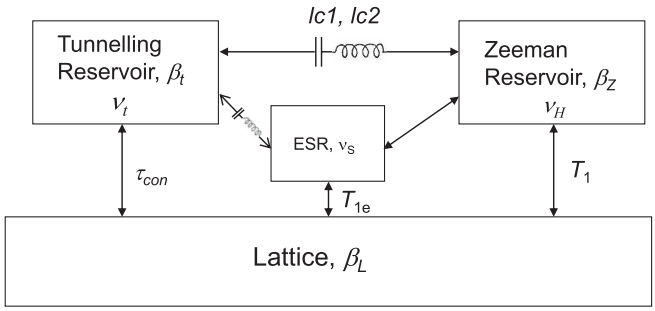

FIG. 6. The thermal reservoir model forms the basis for interpreting the thermodynamics of the CH_3 systems and the simulations of the tunnel resonance spectra. Resonant cross-polarization pathways become available when, by tuning the magnetic field, the tunnel frequency is matched with the Larmor frequency of either a ^{1}H nuclear spin (ν_H) or an electron spin (ν_S). The inverse temperatures of the respective reservoirs are β_Z and β_t

IV. DISCUSSION

Hysteresis is an important feature of tunnel resonance spectroscopy. By incorporating saturation and polarization steps in the pulse sequence, the system can be prepared with a predefined and reproducible Zeeman polarization. However, there is limited scope to control the tunneling polarization in a pre-defined manner. For example, there is no straightforward way to saturate the tunneling polarization. Importantly, there is hysteresis in the system because the state of the tunneling system will depend upon the sequence of experiments that precede an individual measurement in a tunnel resonance scan.

For a methyl group the Zeeman system is characterized by the nuclear spin quartet of total spin 3/2 and the doublet (E_a and E_b) of nuclear spin doublets of total spin 1/2, Fig. 1. Therefore, the heat capacity of the ^{1}H Zeeman reservoir with inverse temperature β_Z is $C_Z \propto h\nu_H[2 \times (\frac{3}{2})^2 + 6 \times (\frac{1}{2})^2]$.

We also identify a thermal reservoir associated with the tunneling states characterized by the energy splitting $\Delta E = h\nu_t$, Fig. 6. The populations of the A and E states define an inverse tunneling temperature β_t which in turn defines a tunneling polarization. Given there are two spatial E states, E_a and E_b, the heat capacity of this reservoir is $C_T \propto h\nu_t[8 \times (\frac{1}{2})^2]$.

At low temperature the tunnel reservoir is normally only weakly coupled to the lattice because thermal equilibration of the A and E spin-symmetry species must be mediated by interactions connecting space and spin variables. At an arbitrary applied B-field, the tunneling and Zeeman reservoirs are similarly decoupled so the manifold of Zeeman-tunneling levels is characterized by the two inverse temperatures, β_z and β_t. However, when the B-field is set to a level-crossing, polarization can efficiently transfer between the tunneling and Zeeman systems leading towards an equilibration of β_z and β_t. This reservoir model is summarized in Fig. 6, showing the resonant cross-polarization links between the Zeeman and tunneling systems.

A. Phenylacetone

The tunnel resonance spectrum of phenylacetone, Fig. 4, is characterized by two steps in polarization which identify the two level-crossings. The field where the ^{1}H NMR signal is recorded, $B_{nmr} = 0.862$ T, lies higher than both level-crossings. In order to access the magnetic field region in between the two level-crossings, the field ramps through lc1 at $B = 0.155$ T during both the downward and upward cycles of the field that span the recovery period at B_r. Therefore, the polarization is determined not only by the evolution that takes place during the recovery period, but also by the level-crossing encounters that initiate cross-polarization between the Zeeman and tunneling reservoirs. Similarly, in the magnetic field region below lc2, $B < 0.077$ T, the system encounters both level-crossings, lc1 and lc2, in each of the downward and upward field cycles that span the recovery period.

There is no facility to restore the tunneling system to a predetermined state before each individual measurement in a scan, so there is hysteresis and the observed ^{1}H polarization is determined by the sequence of events that precede an individual measurement.

The step-like structure in ^{1}H polarization is characteristic and we shall develop a thermodynamic model to explain the tunnel resonance spectrum. At a level-crossing, the following pair of differential equations apply, coupling the Zeeman and tunneling reservoirs,

$$\frac{d\beta_Z}{dt} = -W(\beta_Z - \beta_t)\frac{C_T}{C_T + C_Z},$$
$$\frac{d\beta_t}{dt} = -W(\beta_t - \beta_Z)\frac{C_Z}{C_T + C_Z}, \quad (1)$$

where W is the cross-polarization rate. This is an adaption of an approach developed by Clough *et al.*[16] where it was previously assumed the equilibration of β_Z and β_t is complete and instantaneous. The Zeeman heat capacity C_Z depends on the applied field so $C_Z/C_T = 3/2$ at lc2, whereas $C_Z/C_T = 3$ at lc1. A second feature of the model is that changes in magnetic field are adiabatic so that in field switching from B_i to B_f, the inverse Zeeman temperature changes from β_Z to $(B_i/B_f)\beta_Z$. Finally, the longitudinal polarization follows the usual Bloch dependence during the recovery period,

$$\frac{d\beta_Z}{dt} = -\frac{(\beta_Z - \beta_L)}{T_1^{(B_r)}}, \quad (2)$$

where $T_1^{(B_r)}$ is the spin-lattice relaxation time at the recovery field B_r and β_L is the inverse lattice temperature.

The tunnel resonance experiment in phenylacetone has been simulated according to the above model where the sequence of "measurements" replicated the pulse sequence in Fig. 2. As in the experiment, the recovery field was scanned from high to low values of B_r. In the experiment, the initial tunnelling temperature is not known but, for the purposes of the simulation, at the start of each scan β_t was chosen to be 0.025 K^{-1}. (It was found the choice of initial β_t had little influence on the simulated spectrum.) For each point in the scan the initial ^{1}H polarization is zero due to the saturation pulses that are applied. There is only one adjustable parameter in the simulation, namely, the cross-polarization rate, W. Other parameters are defined by the experimental configuration or

determined by experiment. For example the transit time through each level crossing is estimated from the field ramping rate of the spectrometer (3 $\mathrm{T\,s^{-1}}$) and the width of the peaks that characterize the derivative of the tunnel resonance spectrum, Fig. 4(b). The spin-lattice relaxation time determines the ^{1}H polarization that evolves during the recovery period, τ_r and the field dependence of $T_1^{(B_r)}$ is simply modelled as a linear function extrapolated from T_1 measurements made using a field-cycling pulse sequence at fields above the level crossings, $0.17 < B_r < 0.22$ T.

The simulated tunnel resonance spectra of phenylacetone are shown by the solid lines in Fig. 4(a). Simulations have been conducted for all four spectra where $\tau_r = 90$, 120, 150, 180, and 240 s. The cross-polarization rate constant is $W = 0.65\ \mathrm{s^{-1}}$ and the duration of the level crossing encounters is approximately 4 ms (lc1) and 2 ms (lc2). The thermodynamic model is successful in reproducing the shape of the tunnel resonance spectrum, providing good quantitative agreement with experiment for the height of the step-like features that identify the level-crossings. Furthermore, the level of ^{1}H polarization across the spectrum agrees well with experiment for all recovery times, suggesting the modelled field dependence of $T_1^{(B_r)}$ is a satisfactory approximation within the narrow field range studied.

Evidently the tunnel reservoir is relatively decoupled from the lattice and the tunnel resonance experiment provides no means to measure the lifetime of the A-E tunneling states. No such mechanism was included in the simulations. Direct measurements of the tunneling lifetime have been recently measured for CH_3 groups with tunnel frequencies of order 500 kHz using the dynamic tunneling polarization effect in NMR.[25] In that study, lifetimes were typically of order T_1 suggesting ^{1}H-^{1}H dipolar interactions mediate the thermal equilibration of the tunnel reservoir. In phenylacetone the tunnel frequency is significantly larger than the dipolar frequencies therefore, at fields outside the level crossing regions, it is probable the tunneling lifetime is longer compared with T_1 given the likely magnitude of the spectral density available to drive A-E transitions.

The derivative of the tunnel spectrum, Fig. 4(b), accentuates two additional small features in the tunnel resonance spectrum (dashed arrows). These occur where $\nu_t^{(0)} = 3\nu_H$ and $2\nu_t^{(0)} = 3\nu_H$. The features occur as peaks in the tunnel resonance scan, and as asymmetric features in the derivative. These reveal mechanical coupling between different methyl groups, leading to spin-symmetry species, AA, AE, and EE with total nuclear spin 3, 2, and 1, respectively. They involve double quantum tunneling transitions of the CH_3 rotors. A sketch of the resulting energy levels readily reveals these additional level crossings.[16] That the features appear as peaks in the tunnel resonance spectrum shows the effect of hysteresis is minimal for these features, meaning on fast passage through the level-crossings there is negligible cross-polarization. Only when the field is set for a significant time at the level crossing is the effect on the ^{1}H magnetization manifest. This is consistent with the expectation that double quantum tunneling transitions will be significantly weaker than single quantum transitions.

B. Toluene doped with DPPH radicals

It is a striking to compare the tunnel resonance lineshapes observed in this investigation with the asymmetric peaks commonly observed in the literature.[18–20] The observed tunnel resonances lineshapes in Fig. 5 are symmetric and approximately Gaussian. They have widths of approximately 15 mT, significantly broader than the ESR spectrum of DPPH which has a width of approximately 0.27 mT. This indicates the peak width is intrinsic to the tunneling system. The fact the tunnel resonance peaks are symmetrical indicates there is no spectral diffusion of tunneling energy and hence we conclude that the tunnel peaks in toluene are homogenously broadened.

We shall simulate the tunnel resonances using the model developed in Horsewill and Sun[21] but invoking homogenous broadening of the tunnel peaks. This model is based in turn on Clough and Hobson[18] who described the electron tunnel resonance mechanism. There is resonant contact between the tunneling system and the electron spin mediated by operators such as S_+I_z, S_+I_+, and S_+I_- that define the electron-nuclear dipole-dipole interaction. This has the required symmetry properties to induce a change in CH_3 tunneling state simultaneously with the change in electron spin state. There are three sets of transitions corresponding to the family of spin operators similar to those referred to above; $(\nu_S - \nu_t \pm n\nu_H)$, where $n = 0$, 1. Arising from operators such as S_+I_+ and S_+I_-, the transitions $n = 1$ involve changes in ^{1}H spin polarization, with the ^{1}H Larmor frequency making up any offset between ν_S and ν_t. The electron spins are usually well coupled to the lattice, so the resonant contact leads to a cooling of the tunnel reservoir.

Adapting Clough and Hobson,[18] the rate of change in the ^{1}H polarization mediated by the electron-nuclear dipolar interaction may be written as,

$$\frac{1}{M_0}\left[\frac{dM_z}{dt}\right]_{tr} = a(\beta_L - \beta_t)[W^{(-)}g(\nu_S - \nu_t - \nu_H) - W^{(+)}g(\nu_S - \nu_t + \nu_H)]G(\nu_t). \quad (3)$$

Here, $g(\nu)$ is the electron spin resonance spectrum, $G(\nu)$ is the CH_3 tunneling spectrum, and a is a constant. Additionally the ^{1}H polarization will undergo spin-lattice relaxation making the following contribution to the rate equation for M_z:

$$\left[\frac{dM_z}{dt}\right]_{rel} = -\frac{(M_z - M_0)}{T_1}, \quad (4)$$

where M_0 is the equilibrium polarization at the field B_r and T_1 is the spin-lattice relaxation time at the same field.

The transition $n = 0$ involves no ^{1}H spin flips and hence no change in M_z. However, similar to the transitions $n = 1$, it does induce changes in tunneling state. Therefore, all transitions $n = 0$, 1 lead to a change in the inverse temperature of the tunnel reservoir and adapting Clough and Hobson[18] we

may write,

$$\frac{d(\beta_L - \beta_t)}{dt} = -a_t(\beta_L - \beta_t)\begin{bmatrix} W^{(-)}g(\nu_S - \nu_t - \nu_H) \\ +W^{(+)}g(\nu_S - \nu_t + \nu_H) + W^{(0)}g(\nu_S - \nu_t) \end{bmatrix} G(\nu_t), \quad (5)$$

where $W^{(0,\pm)}$ determine the transition probabilities per unit time and a_t is a constant. This assumes there is spatial diffusion of tunneling energy, but no spectral diffusion.

Equations (3)–(5) provide our model for the electron tunnel resonance and the evolution of M_Z/M_0 and β_t has been simulated according to the tunnel resonance pulse sequence. The ESR spectrum $g(\nu)$ and the tunneling peak $G(\nu)$ are modelled as Gaussians with HWHM 0.27 mT and 6.5 mT, respectively. In the simulation $T_1 = 32$ s, consistent with the value measured at a field close to the tunnel resonance. According to the treatment of Clough and Hobson, the rates $W^{(0,\pm1)}$ have similar magnitude. Because it is observed in experiments that repeated scans through the tunnel resonance do not significantly diminish the tunnel resonance amplitude, we conclude that contact between the electron spin and the CH_3 tunneling system makes only a small perturbation to β_t, influencing the choice of the constant a_t. The value of the constant a is refined to give agreement with the amplitude of the observed tunnel peak.

When $W^{(-1)} = W^{(+1)} = W^{(0)}$ an asymmetric, derivative-like tunnel resonance lineshape is predicted. However, introducing just a 20% difference between $W^{(-1)}$ and $W^{(+1)}$ is sufficient to generate a symmetric Gaussian line, as shown by the solid line in Fig. 5(b). To assess the tunnel resonance lineshapes it has only been necessary to simulate the 6.45 GHz peak since the two CH_3 groups exhibit very similar behavior. The coupling parameters used in this simulation are: $aW^{(-1)} = 7.1 \times 10^{15}\ \mathrm{K\,s^{-3}}$, $aW^{(+1)} = 8.6 \times 10^{15}\ \mathrm{K\,s^{-3}}$, $a_tW^{(0)} = a_tW^{(-1)} = 1.4 \times 10^{12}\ \mathrm{s^{-3}}$, and $a_tW^{(+1)} = 1.6 \times 10^{12}\ \mathrm{s^{-3}}$. The parameters $a_tW^{(0,\pm1)}$ represent an upper limit on the efficiency of the process that cools the tunneling reservoir. Values lower than this threshold give rise to no further significant change in tunnel resonance lineshape but do lead to a reduction in the peak amplitude. In this case, the latter could be offset by making a corresponding increase in the constant a.

The values of $aW^{(\pm1)}$, relating to the changes in ^{1}H polarization arising from contact with the electron spin, are of similar magnitude to those reported for Cu^{2+} doped zinc acetate.[21] However, unlike that study, in the present case there is a 20% asymmetry between $W^{(-1)}$ and $W^{(+1)}$. Furthermore, the cooling of the tunnel reservoir, as reported by the parameters $a_tW^{(0,\pm1)}$, is a much weaker process for DPPH-doped toluene and unlike (Cu^{2+}, Zn) acetate, there is no evidence for spectral diffusion of tunneling energy.

V. CONCLUDING REMARKS

The physics of spin-symmetry eigenstates is one of topical interest with the entanglement of space and nuclear spin degrees of freedom leading to long lived states.[8] In this investigation we have exploited various space-spin interactions to induce resonant coupling between Zeeman and tunneling reservoirs, resulting in effects that are characterized by anomalous features in the magnetic field dependence of nuclear polarization. In the particular tunnel resonances studied here, the polarization changes are modest. However, the study illuminates the underpinning principles. The reservoir model successfully describes the thermodynamics of the two systems which have tunnel splittings differing by three orders of magnitude. By exploiting either nuclear–nuclear or electron-nuclear dipolar interactions as appropriate, analogous ^{1}H nuclear polarization features are observed and quantitative agreement between the simulations and experiment has been achieved.

The tunnel resonance spectra exhibit hysteresis, with an individual measurement in a scan being influenced by the previous cycles to which the sample was subjected. This is particularly well illustrated by the NMR tunnel resonances in phenylacetone which appear as "steps" in ^{1}H polarization. For measurements at fields lower than a level crossing, cross polarization during the passage through the level crossing is unavoidable. This means the observed polarization is characteristic not only of the recovery field, but also of the level-crossing encounter. Only with field-switching rates much faster than the cross-polarization rate could this particular manifestation of hysteresis be avoided.

ACKNOWLEDGMENTS

The field-cycling NMR spectrometer was constructed with the assistance of grants from the Royal Society (Paul Instrument Fund) and the Engineering and Physical Sciences Research Council (GR/R34189/01). A.M.A. and A.A. conducted their work while on sabbatical leave at the University of Nottingham.

[1] W. Press, *Single-Particle Rotations in Molecular Crystals* (Springer-Verlag, Berlin, 1981).
[2] M. Prager and A. Heidemann, Chem. Rev. **97**, 2933 (1997).
[3] A. J. Horsewill, Progr. Nucl. Magn. Reson. Spectrosc. **35**, 359 (1999).
[4] J. Haupt, Phys. Lett. A **38**, 389 (1972).
[5] C. Ludwig, M. Saunders, I. Marin-Montesinos, and U. L. Günther, Proc. Natl. Acad. Sci. U.S.A. **107**, 10799 (2010).
[6] M. Icker and S. Berger, J. Magn. Reson. **219**, 1 (2012).
[7] M. Icker, P. Fricke, and S. Berger, J. Magn. Reson. **223**, 148 (2012).
[8] B. Meier, J-N. Dumez, G. Stevanato, J. T. Hill-Cousins, S. S. Roy, P. Håkansson, S. Mamone, R. C. D. Brown, G. Pileio, and M. H. Levitt, J. Am. Chem. Soc. **135**, 18746 (2013).
[9] C. Beduz, M. Carravetta, J. Y.-C. Chen, M. Concistrè, M. Denning, M. Frunzi, A. J. Horsewill, O. G. Johannessen, R. Lawler, X. Lei, M. H. Levitt, Y. Li, S. Mamone, Y. Murata, U. Nagel, T. Nishida, J. Ollivier, S. Rols, T. Rõõm, R. Sarkar, N. J. Turro, and Y. Yang, Proc. Natl. Acad. Sci. U.S.A. **109**, 12894 (2012).

[10]M. Carravetta, O. G. Johannessen, and M. H. Levitt, Phys. Rev. Lett. **92**, 153003 (2004).
[11]M. Carravetta and M. H. Levitt, J. Am. Chem. Soc. **126**, 6228 (2004).
[12]H. Glättli, A. Sentz, and M. Eisenkremer, Phys. Rev. Lett. **28**, 871 (1972).
[13]P. Van Hecke and G. Janssens, Phys. Rev. B **17**, 2124 (1978).
[14]A. Boekenhoudt and L. Van Gerven, Phys. Rev. B **46**, 5377 (1992).
[15]W. T. Sobol, I. G. Cameron, and M. M. Pintar, Chem. Phys. **152**, 337 (1991).
[16]S. Clough, A. J. Horsewill, and P. J. McDonald, J. Phys. C: Solid State Phys. **17**, 1115 (1984).
[17]S. Clough and B. J. Mulady, Phys. Rev. Lett. **30**, 161 (1973).
[18]S. Clough and T. Hobson, J. Phys. C: Solid State Phys. **7**, 3387 (1974).
[19]S. Clough, A. J. Horsewill, M. N. J. Paley, Phys. Rev. Lett. **46**, 71 (1981).
[20]S. Clough, A. J. Horsewill, and M. N. J. Paley, J. Phys. C: Solid State Phys. **15**, 3803 (1982).
[21]A. J. Horsewill and C. Sun, J. Magn. Reson. **199**, 10 (2009).
[22]A. J. Horsewill, and Q. Xue, Phys. Chem. Chem. Phys. **4**, 5475 (2002).
[23]D. Cavagnat, A. Magerl, C. Vettier, and S. Clough, J. Phys. C: Solid State Phys. **19**, 6665 (1986).
[24]S. Clough, A. Heidemann, A. J. Horsewill, J. D. Lewis, and M. N. J. Paley, J. Phys. C: Solid State Phys. **15**, 2495 (1982).
[25]A. J. Horsewill and S. M. M. Abu-Khumra, Phys. Rev. Lett. **107**, 127602 (2011).